# Investigation of the Mineral Phases of Bone by Solid-State Phosphorus-31 Magic Angle Sample Spinning Nuclear Magnetic Resonance†

A. H. Roufosse, W. P. Aue,‡ J. E. Roberts, M. J. Glimcher,* and R. G. Griffin

ABSTRACT: Phosphorus-31 magic angle sample spinning NMR spectra have been employed to investigate the structure and composition of the mineral deposits in chicken bone. Three different pulse sequences, Bloch decay, cross-polarization, and dipolar suppression, were employed to obtain spectra from bone specimens of varying age. These were compared to the spectra obtained from a variety of crystalline and noncrystalline synthetic calcium phosphate solids used as reference standards. The results suggest that the most suitable model for the major solid calcium phosphate mineral phase in bone is a hydroxyapatite containing ~5–10% $CO_3^{2-}$ and ~5–10% $HPO_4^{2-}$ groups, the latter in a brushite-like configuration. From the NMR line shapes it was deduced that the fraction of $HPO_4^{2-}$ groups was highest in the youngest bone and decreased progressively with increasing age of the specimen.

Despite the fact that the major mineral phase of bone was found by X-ray diffraction to be similar to hydroxyapatite (HA)[1] over 50 years ago (DeJong, 1926; Roseberry et al., 1931), the exact chemical and structural nature of the solid phase(s) of $CaPO_4$ in bone is still unclear (Armstrong & Singer, 1965; Posner, 1969; Termine, 1972; Brown & Chow, 1976; Glimcher, 1976; Glimcher et al., 1981). The difficulty stems in part from the small size of the mineral crystallites in bone, which generate only a few very broad and diffuse X-ray diffraction reflections. This prevents both the unique identification of the major solid phase of $CaPO_4$ and the detection of small amounts of minor $CaPO_4$ components.

The failure of X-ray or electron diffraction to uniquely define structurally or chemically the major calcium phosphate mineral phase in bone or the several minor phases thought to be present as well (Roufosse et al., 1977; Tomson & Nancollas, 1978; Brown et al., 1979; Heughebaert & Montel, 1982) prompted us to examine the short-range atomic order about the phosphate groups in bone mineral by $^{31}P$ MASS NMR. In addition to the standard Bloch decay and dilute spin system cross-polarization experiments (Pines et al., 1973), we have used dipolar suppression of the $^{31}P$ MASS NMR signals when $^1H$ decoupling is removed (Opella & Frey, 1979; Munowitz et al., 1981). These additional data proved to be very important in permitting us to differentiate between several closely related calcium phosphate mineral phases. A comparison of the spectra obtained from various bone samples with those generated by a number of model $CaPO_4$ compounds leads us to conclude that the best available model for bone mineral is a type B CA containing about 5–10% $CO_3^{2-}$ and approximately 5–10% $HPO_4^{2-}$, the latter in a brushite-like (BRU-like) configuration. The fraction of BRU-like $HPO_4^{2-}$ groups decreases with increasing age of the animals. We emphasize that our conclusions are based on a comparison of a finite number of model compounds (Aue et al., 1984) and are therefore not necessarily unique. As more refined models become available, the interpretations may require refinement.

## Materials and Methods

*Preparation of Bone.* The midportions of tibial diaphyses of 17-day-old embryonic chicks and 5-week-, 30-week-, and 1-year-old postnatal animals were used. Tissue was quickly cleaned of soft tissue and periosteum, immediately frozen in liquid nitrogen, lyophilized, and ground to a fine powder in liquid nitrogen (Roufosse et al., 1979).

*Preparation of Synthetic Samples of $CaPO_4$ Solid Phases.* A number of synthetically prepared solid phases of calcium phosphate were used as standards for the $^{31}P$ MASS NMR experiments. Their physical and chemical characteristics are discussed elsewhere (Aue et al., 1984). The samples included monetite (MON) ($CaHPO_4$), brushite (BRU) ($CaHPO_4 \cdot 2H_2O$), highly crystallized hydroxyapatite [$Ca_{10}(PO_4)_6(OH)_2$], octacalcium phosphate (OCP) [$Ca_8H_2(PO_4)_6 \cdot 5H_2O$], amorphous calcium phosphate (ACP), poorly crystalline hydroxyapatite (PCHA) obtained from conversion of a preparation of ACP under strictly controlled conditions (Heughebaert & Montel, 1977), an apatite that contains approximately 12% of its phosphate groups as $HPO_4^{2-}$, a type A carbonatohydroxyapatite (CA), and two type B carbonatohydroxyapatites (CA) containing 3.2 and 14.5% $CO_3^{2-}$, respectively (Aue et al., 1984).

*$^{31}P$ Magic Angle Sample Spinning (MASS) NMR Spectra.* All of the $^{31}P$ NMR spectra were obtained on a home-built pulse spectrometer operating at 119 and 294 MHz for $^{31}P$ and $^1H$, respectively. The radio-frequency field strengths were 13G for protons and 24G for phosphorus. Powdered samples (15–80 mg) were tightly packed into Delrin Andrew–Beams rotors. Spinning rates were 2 kHz to facilitate the comparisons among samples. Chemical shifts are referenced to external 85% $H_3PO_4$.

The pulse sequences employed are described in detail elsewhere (Aue et al., 1984). Four experiments were performed on each sample: (a) proton-decoupled Bloch decay;

† From the Laboratory for the Study of Skeletal Disorders and Rehabilitation, Department of Orthopedic Surgery, Harvard Medical School, Children's Hospital Medical Center, Boston, Massachusetts 02115 (A.H.R., W.P.A., J.E.R., and M.J.G.), and the Francis Bitter National Magnet Laboratory, Massachusetts Institute of Technology, Cambridge, Massachusetts 02139 (W.P.A., J.E.R., and R.G.G.). *Received February 13, 1984; revised manuscript received June 15, 1984.* This research was supported by grants from the National Science Foundation (PCM-8216959), the National Institutes of Health (AM-26843, AM-15671, and RR-00995), and the New England Peabody Home for Crippled Children.

‡ Present address: Biozentrum der Universität Basel, CH-4056 Basel, Switzerland.

[1] Abbreviations: MASS, magic angle sample spinning; NMR, nuclear magnetic resonance; HA, hydroxyapatite; CA, carbonatohydroxyapatite; PCHA, poorly crystalline hydroxyapatite; ACP, amorphous calcium phosphate; OCP, octacalcium phosphate; BRU, brushite; MON, monetite; $CaPO_4$, calcium phosphate solid phase; $PO_4$, phosphate group of unspecified nature (i.e., $PO_4^{3-}$ or $HPO_4^{2-}$ and/or mixtures).

0006-2960/84/0423-6115$01.50/0 

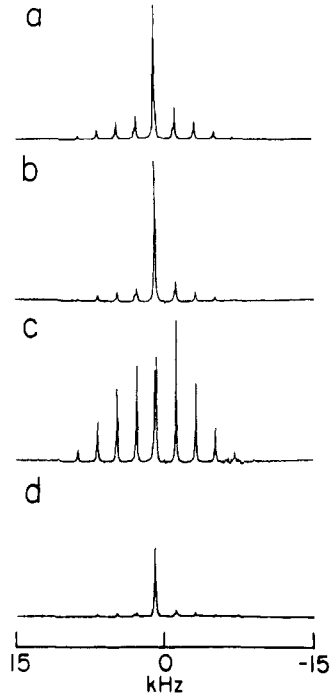


FIGURE 1: Simulated and experimental $^{31}P$ MASS NMR spectra of a 1:1 molar mixture of brushite and crystalline hydroxyapatite: (a) simulation based on a 1:1 integrated intensity ratio; (b) Bloch experiment; (c) proton enhanced; (d) proton enhanced with 0.5-ms dipolar coupling between cross-polarization species and data acquisition. The Bloch decay experiment (b) enhances crystalline hydroxyapatite by a factor of 1.8 over brushite, while the proton-enhanced experiment (c) enhances brushite by a factor of 7.

(b) dilute spin cross-polarization with proton decoupling; (c and d) dilute spin cross-polarization with 0.5 and 1 ms of dipolar suppression (i.e., no proton decoupling) before proton-decoupled data acquisition. Recycle delays were 10 s for the cross-polarization experiments and 60 s for Bloch decays.

*Computer Modeling of NMR Spectra.* In order to examine whether more than one $CaPO_4$ solid phase exists in bone mineral, we employed computer additions of $^{31}P$ MASS NMR spectra from different $CaPO_4$ solid phases in various proportions (Aue et al., 1984). In performing these simulations, it is necessary to adjust the line widths of some of the spectra obtained from synthetic $HPO_4^{2-}$ compounds in order to obtain a facsimile of the spectra obtained from bone. This is accomplished by exponential multiplication of the time-domain signal from a particular synthetic standard, followed by Fourier transformation. It is for this reason that "genuine" noise appears in the spectral simulations illustrated in the figures. To obtain enhancement factors for a particular experiment, both components of the 1:1 integrated intensity spectrum (vide infra) are scaled to match the experimental spectrum, the ratio of the two scaling factors being taken as the enhancement factor.

## Results

The utility of these different pulse sequences for the research described here is illustrated in Figure 1, which demonstrates the theoretical and experimental spectra obtained from the 1:1 molar mixture of HA and BRU. Figure 1a is a theoretical spectrum that consists of a superposition of a HA and a BRU spectrum in a 1:1 $PO_4$ intensity ratio. Specifically, the HA and BRU spectra shown respectively in part 2a of Figure 2 and part 3a of Figure 5 of Aue et al. (1984) were integrated and the intensities scaled to a ratio of 1:1. Therefore, this is the spectrum that would be observed from such a mixture in a decoupled Bloch decay experiment with an infinite recycle delay. The rotational sidebands in this spectrum are due almost exclusively to BRU, since it has a substantially larger shift anisotropy (~130 ppm) than HA (~20 ppm). Moreover, at $\omega_R$ = 2 kHz about 80% of the intensity of BRU resides in the sidebands; the spectrum is dominated by the centerband generated by HA. With a finite recycle delay, 60 s, the HA intensity is enhanced further with respect to BRU as shown in Figure 1b. From spectral simulations, we found the HA to BRU intensity ratio to be 1.8 ± 0.1 under these conditions. All of the synthetic hydroxyapatites we have studied appear to have a shorter $T_1$ values than $CaPO_4$ solid phases containing $HPO_4^{2-}$ groups except for OCP, which contains both $HPO_4^{2-}$ and $PO_4^{3-}$ groups in a mixed lattice. In this instance, the $T_1$ values are more nearly equal. Nevertheless, even in this case, the Bloch decay experiment apparently favors observation of unprotonated phosphates to about the same extent (Aue et al., 1984). Furthermore, it appears that the levels of $HPO_4^{2-}$ found in bone mineral are relatively low (<15% of the total $PO_4^{3-}$ present), and this fact further attenuates the contribution of $HPO_4^{2-}$ to a decoupled Bloch decay spectrum. Therefore, in the discussion below we assume that the Bloch decay spectra include contributions arising almost exclusively from unprotonated, apatite-like phosphate ($PO_4^{3-}$) groups.

It was stated previously (Aue et al., 1984) that the cross-polarization experiment enhances the contributions for $PO_4$ groups that have directly bound and nearby protons. This is illustrated in Figure 1c for the 1:1 HA–BRU mixture. In marked contrast to the Bloch decay spectrum, the cross-polarization spectrum is clearly dominated by the BRU centerband and rotational sidebands. The HA centerband is decreased to about 80% of the BRU centerband, and its sidebands are noticeable only as a slight broadening at the base of the first BRU rotational sidebands. Simulation of this and other cross-polarization spectra indicates that the HA to BRU intensity ratio is 0.14 ± 0.03. The size of this enhancement is quite important in the interpretation of the data obtained in the experiments reported here. As mentioned previously, the $HPO_4^{2-}$ levels in bone are low and would probably be undetectable by $^{31}P$ MASS NMR if this enhancement were 50% smaller. Finally, in Figure 1d we show that insertion of the dipolar-suppression experiment (0.5 ms) selectively attenuates the BRU contribution to the spectrum. After 1 ms of dipolar coupling, the BRU signal is completely suppressed.

In our analyses of the bone spectra, we employed the enhancement factors determined from the spectra of Figure 1 to calculate the amount of $HPO_4^{2-}$ present in the samples. These values must be regarded as estimates, since there are a number of uncontrolled variables that influence these enhancement factors. For instance, cross-polarization is dependent on the strength of the $^{31}P$–$^{1}H$ dipolar coupling, which is a function of the internuclear distance as $r_{PH}^{-3}$. A 10% change in this value results in a 30% change in the strength of the coupling and greatly influences the cross-polarization rate. Furthermore, the proton $T_1$ in synthetic $CaPO_4$'s is most likely governed by the motion of $H_2O$ molecules of hydration. There is no a priori reason to expect these to be identical in biological specimens where the composition and structure are clearly known to be different. Nevertheless, with these reservations in mind we can use the enhancement factors obtained from the spectra of Figure 1 to *estimate* the amount of a $HPO_4^{2-}$ component in the bone mineral samples.

Parts 1–3 of Figure 2 show the $^{31}P$ MASS NMR spectra of bone powder obtained from 17-day-old embryonic chicks and from 5-week-old and 1-year-old postnatal chickens, re-

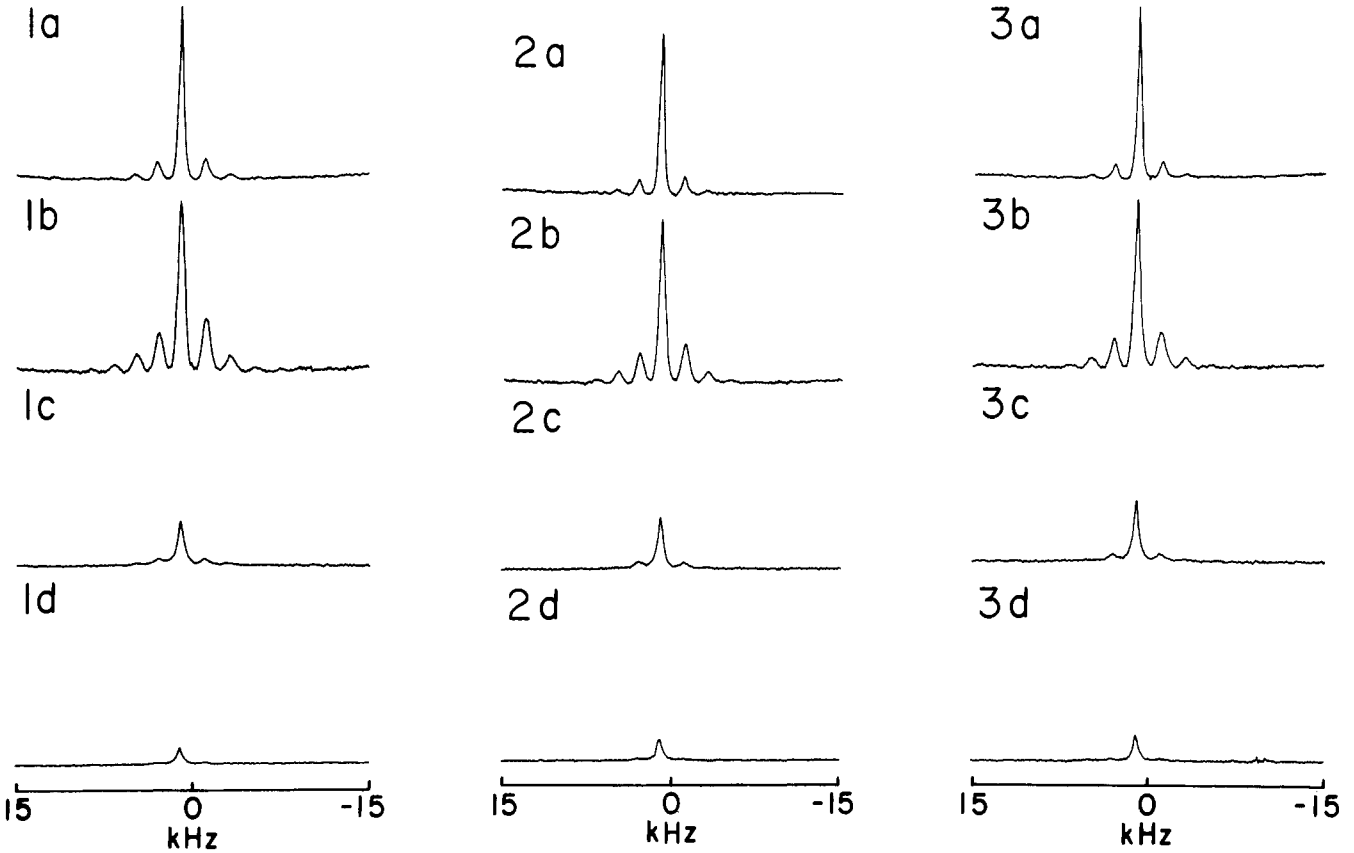


FIGURE 2: $^{31}$P MASS NMR spectra of (1) 17-day-old embryonic chick bone, (2) 5-week-old chick bone, and (3) 1-year-old chick bone. Each column presents data obtained from the four experiments discussed in the text and previous paper: (a) Bloch decay experiment; (b) proton enhanced; (c) proton enhanced with 0.5-ms dipolar coupling between magnetization of the species and data acquisition; (d) same as (c) with a dipolar coupling period of 1 ms. The NMR spectra obtained from 30-week-old chick bone are identical with those shown for 1-year-old chick bone (3). For comparison purposes, all figures present (a) and (b) on the same vertical scale, while (b)–(d) are displayed on an absolute intensity scale.

spectively. Each column has four $^{31}$P NMR spectra corresponding to the NMR experiments described earlier (see Materials and Methods). The $^{31}$P NMR spectra from each of the bone samples consist of one main intense isotropic line flanked by rotational sidebands. None of the NMR spectra in parts 1a,b, 2a,b, and 3a,b of Figure 2 have isotropic chemical shift values and rotational sideband patterns that exactly match the spectra of any of the synthetic standards. These by themselves cannot directly identify the $PO_4$ species in the bone samples. Although the spectra of Figure 2 appear superificially to be quite similar, a closer inspection reveals several interesting differences. First, a comparison of the Bloch decay and cross-polarization spectra (spectra a and b of parts 1–3 of Figure 2) shows that the intensity of the rotational sidebands in the cross-polarization spectra is noticeably stronger. This difference is direct evidence for the presence of protonated $PO_4$ groups. Second, the sidebands in the cross-polarization spectra decrease in intensity relative to the central line with increasing age of the bone mineral. For example, there is a decrease of about 30% in the intensity of the first upper sideband relative to the main isotropic line when one progresses from the 17-day-old embryonic bone to the 1-year-old bone. Third, some intensity of the signal remains after 1 ms of dipolar coupling (Figure 2, parts 1d, 2d, and 3d). These results suggest that there are at least two populations of $PO_4$ groups present in bone mineral. The major population has isotropic and anisotropic chemical shifts and dipolar-suppression behavior similar to the synthetic hydroxyapatites; a minor component yields spectral features similar to $HPO_4^{2-}$.

In Aue et al. (1984), we describe $^{31}$P MASS NMR investigations of a number of synthetic, solid-phase standards of $CaPO_4$ that are relevant to this investigation. The results of these studies show that we can differentiate between most of these synthetic compounds on the basis of their isotropic and anisotropic shifts. Furthermore, when ambiguities exist, these can be partially resolved by the dipolar-suppression technique. For example, apatites exhibit isotropic shifts that are different from compounds containing $HPO_4^{2-}$ groups. In addition, their shift anisotropies are considerably smaller than those observed for protonated $PO_4$ groups. Moreover, since the apatites do not contain large amounts of protonated $PO_4$ groups, their signals are not completely attenuated by the dipolar-suppression experiments. In contrast, BRU and ACP spectra are suppressed completely because they contain $HPO_4^{2-}$ groups and/or water of hydration; e.g., their proton densities are higher. Intermediate between these two cases are MON and OCP, which exhibit partially suppressed spectra. However, in the case of MON, the shift anisotropy is large, and therefore, several strong rotational sidebands are present in the spectrum. Furthermore, within the apatite class of compounds the samples can be arranged in the following order: crystalline hydroxyapatite, hydroxyapatite containing ~12% of its $PO_4$ groups in the form of $HPO_4^{2-}$, poorly crystalline hydroxyapatite, type A carbonatohydroxyapatite, and type B carbonatohydroxyapatites (3.2–14.5% $CO_3^{2-}$). There is in this particular order (i) an increase in the rotational sideband intensities and (ii) a continuous increase in line widths. Furthermore, the signals persist after 1.0 ms of dipolar coupling. From a comparison of these suppression ratios and line widths with those obtained from $^{31}$P MASS NMR spectra of bone, we conclude that the spectra of type B CA containing ~3.2% $CO_3^{2-}$ best approximates the Bloch decay spectra (i.e.,

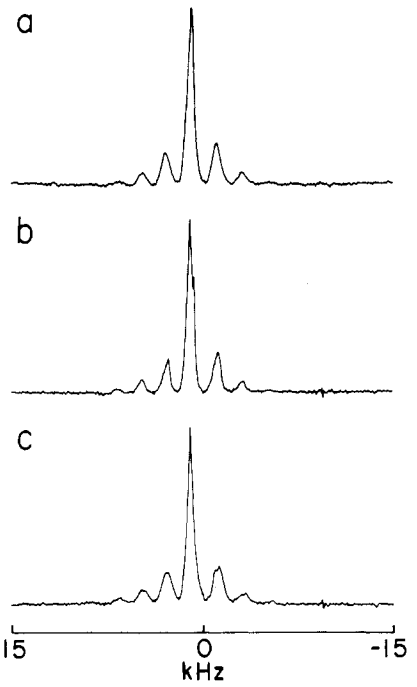


FIGURE 3: (a) Proton-enhanced NMR spectrum of 5-week-old chick bone; (b) simulated NMR spectrum of a mixture of type B carbonatohydroxyapatite (3.2% $CO_3^{2-}$) and 80% octacalcium phosphate; (c) simulated NMR spectrum of a mixture of type B carbonatohydroxyapatite (3.2% $CO_3^{2-}$) and 20% monetite.

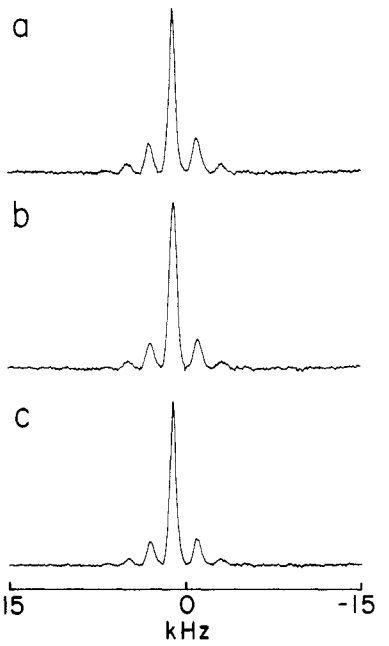


FIGURE 4: (a) Proton-enhanced NMR spectrum of 1-year-old chick bone; (b) proton-enhanced NMR spectrum of amorphous calcium phosphate; (c) proton-enhanced NMR spectrum of a 1:1 mixture of type B carbonatohydroxyapatite (3.2% $CO_3^{2-}$) and amorphous calcium phosphate.

$PO_4^{3-}$) obtained from bone mineral.

It still remains to identify the second $PO_4$ species present in bone mineral that generates the wide sideband pattern and whose contributions to the $^{31}P$ MASS NMR spectra are strongly attenuated by the dipolar-suppression experiments. There are several synthetic standards that appear to be good candidates because one or more features of their NMR spectra (isotropic shift, sideband patterns, and suppression behavior) match those of the second phosphorus ($HPO_4^{2-}$) species found in bone. As shown in Aue et al. (1984), MON, BRU, and OCP are compounds containing $HPO_4^{2-}$ groups, water protons, or both and have $^{31}P$ MASS NMR signals that are suppressed after 1 ms of dipolar coupling. In order to investigate whether one or more of these three compounds are present in bone, we have employed computer additions of their spectra as described above with those of type B CA (3.2% $CO_3^{2-}$) in various proportions.

In Figure 3, we show some typical results obtained from this procedure. Figure 3a shows a proton-enhanced spectrum obtained from bone of 5-week-old animals, and in spectra b and c of Figure 3 are shown simulations obtained by addition of type B CA with OCP and MON, respectively. The spectra shown in Figure 3 are interesting in that the sideband intensities present in the synthetic spectra match those observed in bone quite well. However, there are other differences that suggest that these compounds are probably not significant constituents of bone. First, in the OCP sample a splitting in the centerband remains even after application of 600 Hz of line broadening. We have never observed this type of splitting in the spectra of any of the bone samples. Second, when the centerbands in the simulations are superimposed on the bone spectra, there is a 2 ppm misalignment of the sideband positions. Conversely, superposition of their sideband positions results in the centerbands being misaligned. This results from the differences in the isotropic shifts between OCP and MON and those observed in the bone spectra. Similar differences in centerband positions are observed in comparisons of spectra of these synthetic standards with spectra of 17-day-old embryonic and 1-year-old animals. For these reasons, we do not believe that OCP or MON represents suitable models of the second $PO_4$ species observed in bone mineral.

A third, frequently mentioned possible constituent of bone mineral is ACP, especially in young bone mineral (Harper & Posner, 1966; Eanes et al., 1967; Termine & Posner, 1967). Figure 4 shows a comparison of the proton-enhanced $^{31}P$ MASS NMR spectra of bone from 1-year-old animals (spectrum a) and those obtained from ACP (spectrum b). In this case, both the centerband position and the sideband intensities of the bone spectrum are reproduced quite well in the ACP spectrum. This is a deceptive result for several reasons. Comparison of Bloch decay spectra (not shown) demonstrates the ACP spectra have too much intensity in the sidebands for ACP to be a reasonable model for the major apatitic phase in bone. In addition, we can entirely attenuate the ACP $^{31}P$ MASS NMR spectrum by application of 1 ms of dipolar coupling, whereas the signals from the 1-year-old animal sample persist under the same experimental conditions. This indicates that the ACP must have a higher proton density than the bone mineral and, therefore, does not serve as an appropriate model for the principal or minor component of the bone mineral in 1-year-old animals. However, since ACP has been postulated to be the first mineral phase deposited in bone (Harper & Posner, 1966; Eanes et al., 1967; Termine & Posner, 1967) and would therefore be most likely detected in very young bone, we also compared the spectra of ACP with bone from 17-day-old embryonic animals and from bone of animals of age 5 weeks. In both instances, the two arguments presented above are still valid. Another point concerning the younger bone samples is the second component has a much wider chemical shift anisotropy than ACP (compare part 1b of Figure 2 and Figure 4b). From these arguments, we conclude that ACP cannot account for the second $PO_4^{3-}$ component of the mineral. Figure 4c presents a computer simulation of a 1:1 mixture of ACP and type B CA (3.2% $CO_3^{-}$) for comparison. Again, a reasonable fit with the 1-year-old proton-enhanced spectrum is obtained, although the same three

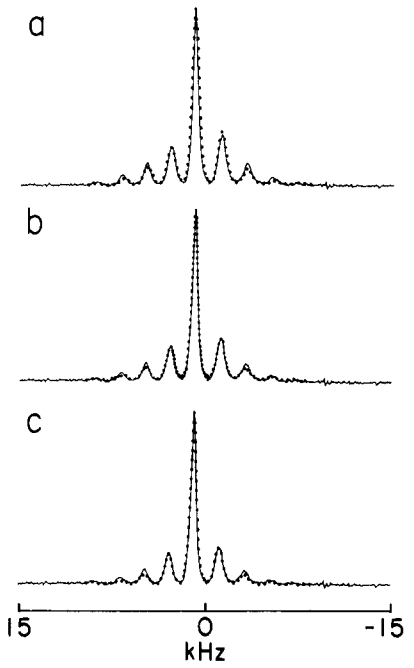


FIGURE 5: (a) Proton-enhanced NMR spectrum of 17-day-old embryonic chick bone (dotted curve), superimposed on a computer simulation of the NMR spectra of a mixture of type B carbonatohydroxyapatite (3.2% $CO_3^{2-}$) and brushite (solid line); (b and c) Similar representations obtained from 5-week-old and 1-year-old chick bone, respectively.

arguments (Bloch decay sideband intensities, dipolar-suppression behavior, and chemical shift anisotropy of the second component in bone) effectively rule out such combinations as models.

Since the spectra shown in Figures 3 and 4 suggest the presence of $HPO_4^{2-}$ groups as the second $PO_4$ phase, we examined the $^{31}$P MASS NMR spectra of a hydroxyapatitic sample containing about 12% of its $PO_4$ groups in the form of $HPO_4^{2-}$. The detailed spectra of this hydroxyapatite sample are shown in Aue et al. (1984). However, the simulations indicate that this compound does not satisfactorily account for the spectra obtained from bone when it is employed either as the major apatite component or as the second species in combination with type B CA.

The most satisfactory results were obtained with brushite. Figure 5 illustrates the results obtained by combining the spectra from type B CA with those of the line-broadened spectra of various proportions of crystalline BRU. In this case, we present the spectra superimposed upon one another so that the reader can inspect the quality of the fit. Figure 5 shows that most of the features of the bone spectra are reproduced with this two component model. First, the centerband position is correct, since BRU, in contrast to OCP or MON, has an isotropic shift that is displaced by 1.4 ppm rather than −1.0 ppm from that of $H_3PO_4$. Second, the intensities of the first two sets of rotational sidebands can be matched exceedingly well by the addition of spectra from these two model compounds. Third, the behavior of the spectra in the proton-suppression experiment is correct. As shown in Aue et al. (1984), the BRU spectrum is completely suppressed after 1 ms of dipolar coupling, whereas some signal remains from the type B CA component. This is exactly the behavior observed in the bone spectra shown in Figure 2. Simulations of the dipolar-suppression time dependence are equally satisfactory. The single discrepancy between the simulations and the spectra is in the intensity of the third set of sidebands. Although these sidebands are observable in the bone spectra, they are not quite as intense as in the simulations. Nevertheless, because of the four factors mentioned, we believe that the best model for the composition of bone mineral from the $^{31}$P MASS NMR data is a type B CA containing ~5–10% $CO_3^{2-}$ and ~5–10% $HPO_4^{2-}$ groups in a BRU configuration.

## Discussion

The $^{31}$P MASS NMR spectra from the $CaPO_4$ mineral phase of chicken bone of four widely different ages all exhibit a strong central line with weak symmetrical sidebands in a Bloch decay experiment. For reasons outlined under Results, we believe this spectrum is due primarily to the hydroxyapatite-like component observed in bone by X-ray and electron diffraction. In the cross-polarization experiments, the intensity of the centerband relative to the rotational sidebands is decreased, and the sideband patterns become asymmetric. Furthermore, when 1 ms of dipolar coupling is inserted into the experiment, a significant fraction of the signal from the bone samples remains. By use of spectral simulation techniques, the cross-polarization spectra can be reproduced with a two-component model consisting of type B CA and a line-broadened brushite spectrum. This model reproduces the centerband and sideband intensities and is also consistent with the dipolar-suppression experiments. No other synthetic crystalline or amorphous calcium–phosphorus standard singly or in such combinations reproduces all of the features of the $^{31}$P MASS NMR spectra obtained from bone.

The suggested ~5–10% content of $CO_3^{2-}$ in the CA of bone can only be considered as an average value since the $CO_3^{2-}$ content of bone mineral increases as a function of age (Biltz & Pellegrino, 1977). Had they been available to us, we would have liked to have examined a series of type B carbonatoapatites with $CO_3^{2-}$ contents ranging from approximately 3 to 15% and to have compared these spectra with those of a large series of bone mineral specimens over a wide range of ages. Such experiments are currently under way.

The detection of $HPO_4^{2-}$ groups in a brushite-like configuration in samples of bone by $^{31}$P MASS NMR is consistent with chemical analyses that have consistently demonstrated the presence of acid phosphate moieties in bone mineral (Pellegrino & Blitz, 1972; Dallemagne & Richelle, 1973). Moreover, highly crystalline BRU ($CaHPO_4 \cdot 2H_2O$) has been detected by X-ray diffraction as a component of the earliest mineral phase of chick bone (Roufosse et al., 1979). However, in more recent studies, it has not been possible to demonstrate the presence of *crystalline* brushite in similar samples with similar techniques (Bonar et al., 1984). It therefore appears that the *crystalline* brushite reported as a component in chick bone and in other tissues (Munzenberg & Gebhardt, 1969; Betts et al., 1979; Glick, 1981) probably arose from the crystallization of $HPO_4^{2-}$ groups. At the moment, it is unclear why the brushite-like $HPO_4^{2-}$ groups detected by $^{31}$P MASS NMR do not generate a coherent X-ray diffraction pattern similar to that observed for crystalline brushite (Bonar et al., 1984).

Neither chemical analyses nor the $^{31}$P MASS NMR data provide any information as to whether the $HPO_4^{2-}$ groups in the brushite configuration are spatially and physically part of the major extracellular mineral particles of bone or they are constituents of other extra- or intracellular mineral particles spatially separated and distinct from the major extracellular mineral phase of bone. If the $HPO_4^{2-}$ groups are indeed physically part of the major HA mineral particles in the extracellular tissue spaces, they could be located on the surface or within the crystallites in domains too small to diffract coherently by X-ray or electron diffraction.

The failure to detect significant amounts of ACP by $^{31}P$ MASS NMR in even the very young embryonic bone, which contains a large proportion of newly deposited bone mineral, is consistent with recent results obtained by X-ray diffraction radial distribution function analyses (Glimcher et al., 1981; Grynpas et al., 1984). These data effectively rule out the possibility that ACP is the major solid phase of $CaPO_4$ of newly deposited bone mineral (Harper & Posner, 1966; Eanes et al., 1967; Termine & Posner, 1967). The simulations of ACP and type B CA (3.2% $CO_3^{2-}$) demonstrate that some features of the 1-year-old bone spectra can be reproduced with ACP spectra. However, examination of the spectra from younger bone specimens, where ACP was predicted to occur (Harper & Posner, 1966; Eanes et al., 1967; Termine & Posner, 1967), confirms that ACP is not a significant portion of bone mineral for three reasons. First, the enhancement behavior of the rotational sidebands (Bloch decay vs. proton-enhanced experiments) in spectra obtained from ACP does not mimic that observed from the bone samples. Second, the dipolar-suppression characteristics of ACP are incorrect. Finally, the anisotropic chemical shift of ACP is too small to account for the wide rotational sideband patterns assigned to brushite-like $HPO_4^{2-}$ groups. Because several preparations of ACP yield nearly identical NMR spectra (Aue et al., 1984), we can state that these synthetic ACP preparations are not present in bone in amounts >5%.

The $^{31}P$ MASS NMR spectra are also observed to be a function of the age of the animal and of the age of the bone mineral. Although the changes are not large, they are reproducible and suggest that the proportion of the hydroxyapatite-like component increases relative to the $HPO_4^{2-}$ groups in a brushite configuration with increasing age and maturation. The proportion of the two components at any given age is difficult to determine with certainty because the enhancement factors are a strong function of a number of variables that cannot be controlled in the biological specimens. For example, the proton $T_1$ values, the proton density in the microdomains present in bone, and the proximity of protons to the $PO_4^{3-}$ groups are all factors that are unknown. However, if we assume that the relative enhancement factors observed in crystalline HA and BRU are applicable to bone mineral, the ratio of brushite-like $HPO_4^{2-}$ groups to HA is calculated to be 0.12, 0.08, and 0.05, all ±0.03, for the bone from the 17-day-old embryo and the 5-week-old and 1-year-old postnatal animals, respectively. In general, 5–10% of the $PO_4$ groups in bone mineral appear to be in a brushite-like configuration.

In conclusion, we have shown that it is possible to exploit solid-state $^{31}P$ MASS NMR techniques to differentiate and identify $PO_4$-containing crystalline and amorphous mineral phases. This was achieved in part by employing pulse sequences that alter the contribution of specific types of $PO_4$ groups to the spectrum. This type of approach is likely to have many potential applications in other studies of components of biological tissues and organs in the solid state, particularly to identify components, which, for a variety of reasons, cannot be adequately identified by conventional X-ray diffraction techniques.

**Registry No.** MON, 21063-37-6; BRU, 14567-92-1; CA, 66524-19-4; OCP, 14096-86-7; HA, 1306-06-5; $HPO_4^{2-}$, 29505-79-1; calcium phosphate, 10103-46-5.

## References


Armstrong, W. D., & Singer, L. (1965) *Clin. Orthop. 38*, 179.

Aue, W. P., Roufosse, A. H., Glimcher, M. J., & Griffin, R. G. (1984) *Biochemistry* (preceding paper in this issue).

Betts, F., Trotta, R., Goldberg, M. A., & Posner, A. S. (1979) *Trans. Orthop. Res. Soc. 4*, 117.

Biltz, R. M., & Pellegrino, E. D. (1977) *Clin. Orthop. 129*, 279.

Bonar, L. C., Grynpas, M. D., & Glimcher, M. J. (1984) *J. Ultrastruct. Res. 86*, 93.

Brown, W. E., & Chow, L. C. (1976) *Annu. Rev. Mater. Sci. 6*, 213.

Brown, W. E., Schroeder, L. W., & Ferris, J. S. (1979) *J. Phys. Chem. 83*, 1385.

Dallemagne, M. J., & Richelle, L. J. (1973) in *Biological Mineralization* (Zipkin, I., Ed.) p 23, Wiley, New York.

DeJong, W. F. (1926) *Recl. Trav. Chim. Pays-Bas 45*, 445.

Eanes, E. D., Termine, J. D., & Posner, A. S. (1967) *Clin. Orthop. 53*, 223.

Glick, P. L. (1981) in *The Chemistry and Biology of Mineralized Connective Tissues* (Veis, A., Ed.) p 309, Elsevier/North-Holland, New York.

Glimcher, M. J. (1976) in *Handbook of Physiology: Endocrinology* (Greep, R. O., & Astwood, E. B., Eds.) Vol. 7, pp 25–116, American Physiological Society, Washington, DC.

Glimcher, M. J., Bonar, L. C., Grynpas, M. D., Landis, W. J., & Roufosse, A. H. (1981) *J. Cryst. Growth 53*, 100.

Grynpas, M. D., Bonar, L. C., & Glimcher, M. J. (1984) *Calcif. Tissue Int. 36*, 291.

Harper, R. A., & Posner, A. S. (1966) *Proc. Soc. Exp. Biol. Med. 122*, 137.

Heughebaert, J.-C., & Montel, G. (1982) *Calcif. Tissue Int. 34*, S103.

Munowitz, M., Griffin, R. G., Bodenhausen, G., & Huang, T. H. (1981) *J. Am. Chem. Soc. 103*, 2529.

Munzenberg, K. J., & Gebhardt, M. (1969) *Dtsch. Med. Wochenschr. 25*, 1.

Opella, S. J., & Frey, M. H. (1979) *J. Am. Chem. Soc. 101*, 5854.

Pellegrino, E. D., & Biltz, R. M. (1972) *Calcif. Tissue Res. 10*, 128.

Pines, A., Gibby, M. J., & Waugh, J. S. (1973) *J. Chem. Phys. 59*, 569.

Posner, A. S. (1969) *Physiol. Rev. 49*, 760.

Roseberry, H. H., Hastings, A. B., & Morse, J. K. (1931) *J. Biol. Chem. 90*, 395.

Roufosse, A. H., Sabine, W. K., Landis, W. J., & Glimcher, M. J. (1977) *Trans. Orthop. Res. Soc. 2*, 87.

Roufosse, A. H., Landis, W. J., Sabine, W. K., & Glimcher, M. J. (1979) *J. Ultrastruct. Res. 68*, 235.

Termine, J. D. (1972) *Clin. Orthop. 85*, 207.

Termine, J. D., & Posner, A. S. (1967) *Calcif. Tissue Res. 1*, 8.

Tomson, M. B., & Nancollas, G. H. (1978) *Science (Washington, D.C.) 200*, 1059.